Optical study of the metal-semiconductor transition in $BaPb_{1-x}Bi_xO_3$

S. Tajima, S. Uchida, A. Masaki, H. Takagi, K. Kitazawa, and S. Tanaka
Department of Applied Physics, University of Tokyo, Hongo 7-3-1, Bunkyo-ku, Tokyo 113, Japan

A. Katsui
Ibaraki Electrical Communication Laboratory, Nippon-Telegram-Telephone Company, Tokaimura, Naka-gun, Ibaraki-ken 319-11, Japan

(Received 24 June 1985)

The reflectivity spectra of the $BaPb_{1-x}Bi_xO_3$ alloy series are investigated over a wide energy range, 20—30 000 cm^{-1}, and over the whole compositional range. As the Bi composition x is increased, the position of the plasma edge is found to shift to higher energy corresponding to an increase in the electron density contributed by the Bi atoms. With further increase in x we find that the spectrum deviates from the usual Drude behavior. From a Kramers-Kronig analysis we infer that a pseudogap, or a minimum in the density of states, develops with x. The pseudogap arises from the trend towards splitting of the Bi-derived band and transforms to a real gap at the metal-semiconductor transition $x_c \simeq 0.35$. The gap formation is supposed to be due to the presence of the short-range order of the Bi charge disproportionation state. Anomalous electronic transport properties observed in the metallic phase are well explained by assuming this pseudogap near the Fermi level.

I. INTRODUCTION

Ever since the high-T_c superconductivity of $BaPb_{1-x}Bi_xO_3$ was discovered by Sleight *et al.*,[1] many efforts have been made to determine the origin of the high T_c for non-transition-element compounds.[2] Gradually the following facts have been revealed. The high T_c is attributed to an extraordinarily strong electron-phonon interaction, related to some soft phonons.[3] One of the plausible candidates for the origin of these phonons is the breathing mode, which is the contraction and expansion of the oxygen octahedra around the Bi or Pb atoms.[4] Its softening is due to the fact that the Bi atom has two stable ionic states (Bi^{3+} and Bi^{5+}), which makes the valence of the Bi atom liable to fluctuate even in the Pb^{4+} matrices. In $BaBiO_3$ this mode is considered to be completely softened and static displacements of the oxygen atoms appear, making the material semiconducting. The resistivity measurements revealed that the metal-semiconductor (M-S) transition takes place at about the composition $x \simeq 0.35$.[1,5]

A few fundamental problems remain unsolved as yet. (i) What are the electronic states or the band structure of this material? (ii) How is the high-T_c superconductivity related to the M-S transition? (iii) What are the characteristics of the charge disproportionation? Does the breathing-mode phonon freeze out also in the alloys? For the semiconductors phase only, we have recently obtained evidence showing that the breathing-mode phonons are frozen out.[6] Specifically, one needs to explain the following unusual properties. (i) The resistivity increases with decreasing temperature for the metallic samples with $x > 0.15$.[7,8] (ii) The carrier density estimated from the Hall effect seems to saturate when x exceeds 0.2.[5,8] (iii) The density of states at the Fermi energy estimated from the Seebeck coefficient and the specific heat is reduced from the expected value of the normal metal for $x > 0.2$.[9,10] The purpose of the present work is to find a model for the electronic structure of this alloy series which can explain the above properties.

Most previous works were on powder or polycrystalline specimens. Thus, we could not rule out the possibility that some of the unusual properties in this material might be due to the presence of the polycrystalline boundaries. Recently, single crystals have been successfully grown in some laboratories[7,11] and almost the same properties are also observed in the single crystals.[7,8,12] Therefore we should regard the singularities as intrinsic to this material.

Several theories have been proposed so far to explain the M-S transition. The band structure calculated by Mattheiss and Hamann with the linearized—augmented-plane-wave (LAPW) method explains well, most of the properties in the metallic phase but does not work so well in the semiconducting phase or in the M-S transition range.[4] According to their charge-density-wave— (CDW) like image the energy gap can appear only near $x = 1.0$, whereas semiconducting properties have been observed to persist over a wide range: $0.35 < x \leq 1.0$. Kondo and Hanamura proposed a model in which the semiconductivity can be explained up to a Pb concentration of about 30 at. %, by taking account of the site-energy difference between Pb and Bi.[13] Rice and Sneddon interpreted the semiconductivity of $BaBiO_3$ as due to the real-space electron pairing which gives rise to the valence configuration $Ba_2Bi^{3+}Bi^{5+}O_3$, by introducing the concept of Anderson's negative U.[14] They concluded that the M-S transition takes place as Pb dilutes the Bi^{3+}-Bi^{5+} superlattice and weakens the real-space pairing. The model proposed by Yoshioka and Fukuyama considers both the site energy difference and the on-site attractive interaction between

electrons.[15] Choosing reasonable parameters, they explained the semiconductivity as well as the superconductivity of this system.

There have been few experimental attempts to determine the electronic structure and/or the mechanism giving rise to the *M-S* transition of this material. For the investigation of the *M-S* transition, optical methods are suitable tools. Many optical studies have been successfully performed on materials such as TaS_2 and $TaSe_2$ in which a charge-density wave is formed[16] or on materials, such as V_2O_3, in which the Mott transition occurs.[17] Nevertheless, little optical investigation has been made on $BaPb_{1-x}Bi_xO_3$ except for a few works—the infrared-absorption measurements of de Hair and Blasse[18] and of Khan *et al.*[19] Khan *et al.* observed optically the *M-S* transition at the composition $x=0.4$ and estimated the energy gap of $BaBiO_3$ at about 0.1 eV from the extrapolated absorption edge.

We have carried out reflectivity measurements over a wide energy range. We have observed the phonon structure by far-infrared optical and Raman scattering measurements and the plasma excitation in the visible and near infrared region. The results of the former two experiments are reported elsewhere.[6,20] In our preliminary report[21] the reflectivity spectra of the polycrystalline specimens with metallic composition $x=0$—0.25 were shown and the electron effective mass was estimated from the observed plasma frequency. In the present work we study mainly the plasmon behavior determined from the reflectivity spectra of polycrystalline samples and single crystals over the whole compositional range of $BaPb_{1-x}Bi_xO_3$, paying particular attention to the *M-S* transition.

In Sec. II a brief description of the method of crystal growth and the setup used for the optical measurement is presented. The reflectivity spectra are shown in Sec. III, along with the results of curve fitting by the Drude equation and of the Kramers-Kronig transformation for the reflectivity spectra. In Sec. IV on the basis of our experimental results the band scheme of this material is built up systematically for three composition regions—the metallic region near $BaPbO_3$, the semiconducting region near $BaBiO_3$, and the transition region between the two. Moreover, the relevance to the theories proposed so far is discussed and our speculation on the *M-S* transition and the electronic structure of this material is presented. Finally we summarize our investigation in Sec. V.

II. EXPERIMENT

The polycrystalline samples used for the present measurement were sintered, prepared by the hot-press method.[5] Their compositions x were 0, 0.05, 0.125, and 0.2. Although there were pores in the samples, the fraction of the total volume seemed to be less than 10%. The single crystals were grown by the flux method in which $PbO_2 + Bi_2O_3$ was used as a solvent. The crystallization method has been described in detail in Ref. 11. The compositions of the single crystals were 0.17, 0.20, 0.27, 0.33, 0.4, 0.5, 0.6, and 1.0. These compositions were determined by an electron-probe microanalyzer, using the polycrystalline standard samples as references, because the composition of the crystals might possibly have been a little different from the initial compositions of the melt. The samples with composition in the range $0 \leq x \leq 0.35$ are dark bronze in color. The color becomes reddish in the range $0.35 < x < 0.8$ and golden in the range $x \geq 0.8$. This change seems to suggest that optically detectable change in the electronic structure takes place as x increases.

All the samples except the as-grown $BaBiO_3$ sample were mirror polished before the optical measurements by using Al_2O_3 powder of 0.06 μm in size. The mirror of the evaporated Ag films was used as a reference in order to determine the absolute value of the reflectivity.

The reflectivity spectra in the wavelength range $\lambda=0.4$—2.5 μm were measured by using a Perkin-Elmer grating-type spectrometer with a photomultiplier detector for $\lambda=0.4$—0.7 μm and a PbS detector for $\lambda=0.7$—2.5 μm. The infrared spectra in the longer-wavelength range $\lambda=2.5$ μm (40 000 cm^{-1})—500 μm (20 cm^{-1}) were measured by using a Fourier-type spectrometer with a Ge bolometric detector. The reflectivity data obtained were analyzed by computer calculation.

III. RESULTS AND ANALYSIS

A. Reflectivity spectra

The reflectivity spectra of the end members of this alloy series are shown in Fig. 1. The spectra of $BaPbO_3$ and $BaPb_{0.95}Bi_{0.05}O_3$ are typical for metals, having a high-reflectivity region due to the screening effect of the free electrons and a reflectivity edge, the so-called plasma edge. In $BaBiO_3$ the reflectivity is relatively low over the whole spectral range and the phonon structure appears clearly, corresponding to the disappearance of the free electrons. It is evident from this spectrum that $BaBiO_3$ is a semiconductor.

Now we compare the spectra of the samples with the intermediate compositions. In Fig. 2 we reproduce the result of Ref. 21, where the spectra of the polycrystalline samples are shown at compositions $x=0$—0.25 in the wavelength range $0.7 \leq \lambda \leq 2.5$ μm,[21] in which the in-

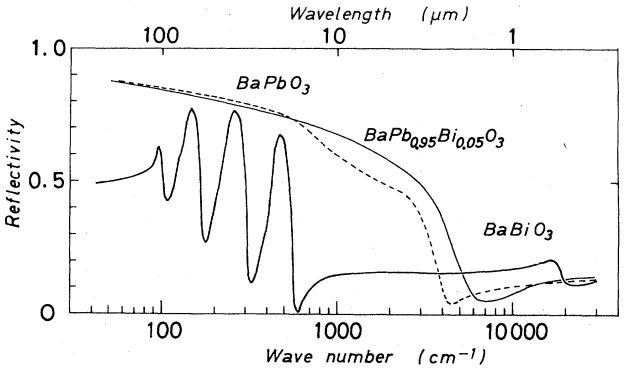

FIG. 1. Reflectivity spectra of $BaPb_{0.95}Bi_{0.05}O_3$ (typical metal) and $BaBiO_3$ (typical semiconductor). The dashed line is the spectrum of $BaPbO_3$ (semimetal).

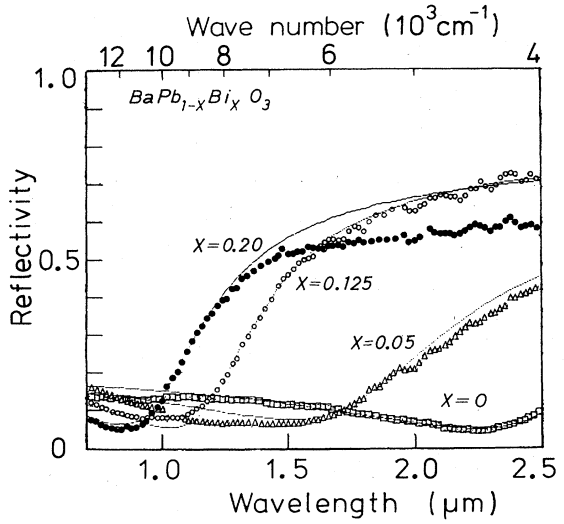

FIG. 2. Reflectivity spectra of the polycrystalline samples in the compositional range $0 \leq x \leq 0.2$. The solid curves are the results of the Drude fit using Eq. (1).

teresting spectral change of the plasma reflection can be observed. As seen in the figure, the plasma edge shifts towards higher energy as the Bi content increases. The solid lines in the figure are the fitting curves calculated by using the Drude equation as follows:

$$\epsilon(\omega)=\epsilon_\infty\left[1-\frac{\omega_p^2}{\omega^2+i\omega\gamma}\right], \tag{1}$$

where ω_p is the plasma frequency, γ is the damping factor of this excitation, and ϵ_∞ is the optical dielectric constant. For the samples of $x=0$, 0.05, and 0.125 the experimental curves can be fitted fairly well to the calculated curves, which indicates that these samples are normal metals. However, for the sample with $x=0.20$ the experimental curve shows a deviation from the Drude curve in the lower-energy region.

This anomalous behavior is also observed in the spectra of the single-crystalline samples with $x \geq 0.17$ as shown in Fig. 3. The solid curves in the figure are the Drude curves, and the arrows indicate the position of ω_p obtained by the fitting. When the Bi content x increases, the plasma edge shifts towards higher energy while the reflectivity in the lower-energy region is reduced more and more and the deviation from the Drude curve becomes accordingly more remarkable.

In Fig. 3 the spectrum seems to change continuously from the metallic to the semiconducting phase, and the boundary composition between these two phases is not clear. Comparing the spectrum of $BaPb_{0.67}Bi_{0.33}O_3$ with that of $BaPb_{0.6}Bi_{0.4}O_3$ shown in Fig. 4, we can see the clear difference between the two in the low-temperature spectra. In $BaPb_{0.6}Bi_{0.4}O_3$ the phonon structures manifest themselves as a consequence of the reduction of the number of thermally excited free electrons, whereas we see no appreciable change in the spectrum of $BaPb_{0.67}Bi_{0.33}O_3$

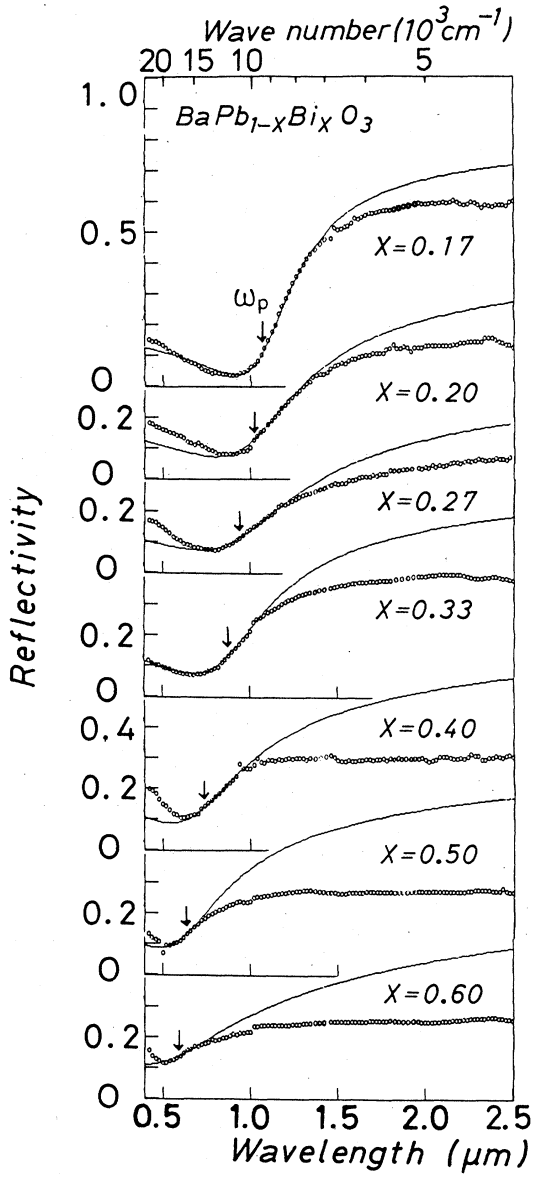

FIG. 3. Series of reflectivity spectra of the single-crystalline samples in the compositional range $0.17 \leq x \leq 0.06$. The solid curves are the results of the Drude fit. The arrows indicate the wavelength positions of the plasma edges.

after cooling down the sample. Consequently, we can state that the *M-S* phase boundary is located at a composition between 0.33 and 0.4, in agreement with the results of the resistivity measurement.[5] It is surprising that although the samples with $x \leq 0.33$ are "metals," their spectra show such a large deviation from the Drude curves as shown in Fig. 3. The lowest composition at which this anomaly sets in is not clear because no single crystals are available at present in the compositional range $x < 0.17$. However, it shows up at least at $x=0.17$ and above.

Concerning the origin of this anomaly in the spectra, one may suggest the possibility that the samples are not

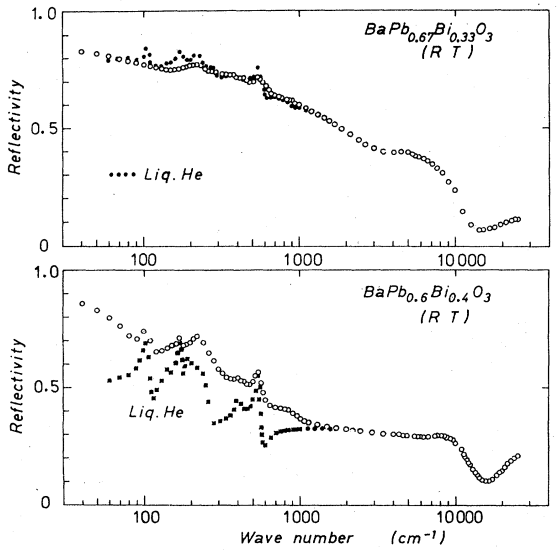

FIG. 4. Comparison of the reflectivity spectrum of $BaPb_{0.67}Bi_{0.33}O_3$ with that of $BaPb_{0.6}Bi_{0.4}O_3$. The difference between them can be observed at the liquid-helium temperature.

homogeneous as pointed out by Methfessel and Methfessel.[22] In the alloy system there are always possibilities of either segregation or phase separation. In particular, phase separation is often an inevitable consequence for a system which shows a M-S transition upon changing the alloy composition. If such a phase separation were to take place in the present crystals, the samples near the critical composition ($x_c \simeq 0.35$) would be a macroscopic mixture of the metallic and semiconducting domains. In such a case the reflectivity should be

$$R(\omega)=(1-f)R_M(\omega)+fR_S(\omega)\ , \tag{2}$$

where f is the volume fraction of the semiconducting domain and R_M and R_S are the reflectivity in the metallic and semiconducting domains, respectively. By calculating R_M from Eq. (1) and setting R_S constant as shown in the spectrum of $BaBiO_3$, we can obtain a good fit to the experimental spectrum. It is reasonable that the obtained parameter f, is an increasing function of x. However, in the usual phase separation the composition of the individual phases should be fixed and as a result, the plasma edge should be observed at the same frequency even if the reflectivity decreases with increasing x, whereas our experimental results show a continuous shift of the edge with x. Moreover, neither the x-ray or the transmission-electron-microscope observation could detect any secondary phase present in our samples.[8] Thus, we regard the present alloy series as a macroscopically homogeneous system.

B. Analysis

Regarding our samples as macroscopically homogeneous, we have carried out the Kramers-Kronig transformation for the experimental spectra in order to make clear

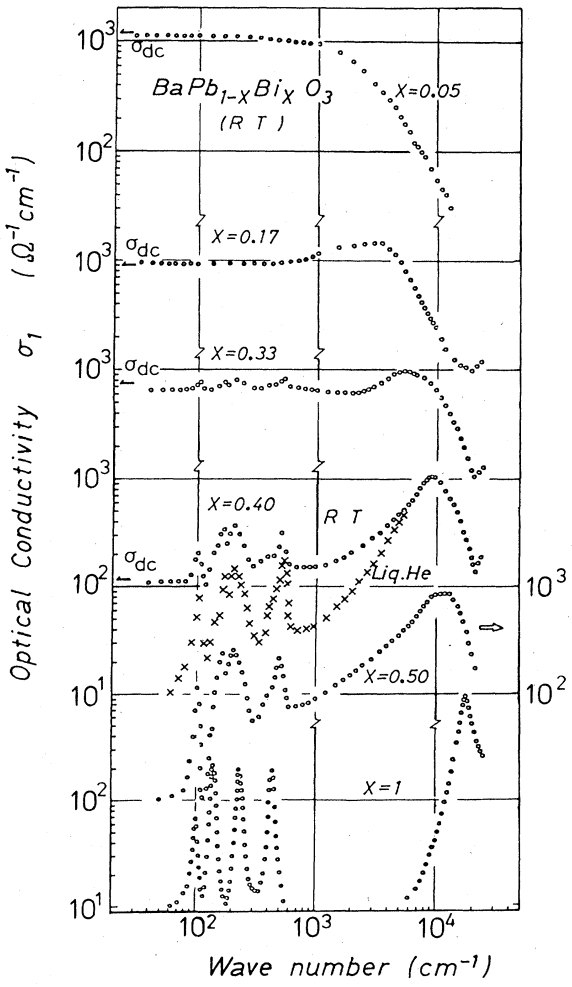

FIG. 5. Real part of the optical conductivity σ_1 for various compositions of $BaPb_{1-x}Bi_xO_3$ which are obtained from the calculation of Kramers-Kronig transformation for the reflectivity spectra.

the mechanism of the anomalous spectral behavior. From the dielectric function obtained $\epsilon=\epsilon_1+i\epsilon_2$, the real part of the conductivity σ_1 is calculated as shown in Fig. 5, by using the relation $4\pi\sigma_1(\omega)=\omega\epsilon_2(\omega)$. Concerning the accuracy of the calculation, we have the following problem. Although the spectral range covered in our measurement is from 20 cm^{-1} ($\sim$2 meV) to 25 000 cm^{-1} ($\sim$3 eV), we need a still wider range to take into account all of the electronic excitations. Actually there seems to be one more electronic excitation at an energy higher than 3 eV. In order to see the influence of the extrapolation procedure the calculations have been done by varying the constant value of R extrapolated above 25 000 cm^{-1} or by adding an oscillator centered around 40 000 cm^{-1} with various oscillator strengths. Below 20 cm^{-1} different extrapolation schemes were also used. It turns out that these procedures do not seriously affect the results in the energy range of interest. As shown in Fig. 5 the extrapolated dc values of the optical conductivity are in good

agreement with the values obtained from the transport measurement, which is part of the evidence that the accuracy of the present calculation is acceptable.

The spectrum of the sample at $x=0.05$ is a typical one expected from the Drude theory. On the other hand, in the semiconducting phase for $x>0.35$ the conductivity in the lower-energy region is reduced considerably and the phonon structure dominates in this spectral region. In the higher-energy region a distinct peak characterizes the spectrum as is typically shown in the case of $BaBiO_3$. This can be assigned to an electronic transition across an energy gap in the semiconducting bands, the position of which corresponds approximately to the value of the energy gap. When x increases, this spectral peak sharpens and its position shifts towards higher energy. The energy corresponding to the peak position is plotted against the Bi composition x in Fig. 6. It is notable that even in the metallic phase the optical conductivity in the lower-energy region reduces gradually with increasing x and as a result, a peak appears in the spectrum. This peak has already manifested itself in the spectrum at $x=0.17$. Thus, the conductivity spectrum seems to change continuously from a typical metallic one to a semiconducting one with increasing x. Observing this spectral change, we can interpret the reflectivity reduction in the lower-energy region as the transfer of the low-energy conductivity to the high-energy peak and the shift of its position towards higher energy.

In contrast to the spectra in the lower-energy region, the higher-energy spectra ($\omega>\omega_p$) can be explained relatively well by the Drude theory. As shown by the arrows in Fig. 3, the plasma edge shifts continuously with x. The values of ω_p^2 obtained by the curve fitting are plotted against the composition x in Fig. 7. (For the semiconducting samples at $x>0.4$ the plotted values were obtained by the curve fit using the other form of the dielectric function as described in Sec. IV because the Drude fit loses its significance. There was no distinct difference between the values obtained by these two curve fittings.) ω_p^2 increases almost linearly with x over the whole compositional range except at $x=1.0$. As the carrier density n involved in the optical excitation is presumed to be almost equal to the Bi concentration, this behavior of ω_p seems to confirm the relation between ω_p and n as

$$\omega_p^2=\frac{4\pi ne^2}{m^*\epsilon_\infty}, \tag{3}$$

where m^* is the electron effective mass. Hence, we can say that the electrons contributing to the collective excitation of this material are supplied by the substituted Bi atoms. The value of ϵ_∞ obtained by the curve fitting is almost constant (~ 5) over the compositional range at least up to $x=0.6$. As suspected in Figs. 2 and 3, another electronic excitation may exist in the energy region above 3 eV (25 000 cm^{-1}). Since the optical dielectric constant ϵ_∞ includes the contribution of such higher-energy excitations, it can no longer be regarded as a constant when ω_p comes near this excitation energy. We have checked the influence of the higher-energy excitation on the value of ω_p by adding one more oscillator with excitation energy $\omega_G=35\,000$ cm^{-1} and oscillator strength $S=0.64$: The best-fit parameters obtained are $\hbar\omega_p=2.14$ eV and $\epsilon_\infty=4.2$ for $x=0.6$ as compared to the results without this additional oscillator, $\hbar\omega_p=2.07$ eV and $\epsilon_\infty=5.0$. For $BaBiO_3$ the presence of the higher-energy excitation affects the fitting parameters more seriously, making the data point in Fig. 7 shift upwards appreciably. However, we can say from Fig. 7 that ω_p^2 increases linearly with x at least up to about $x=0.5$ and this good linearity suggests that the optical effective mass does not vary so much with x.

The carrier densities estimated from the Hall effect[8] and those calculated on the assumption that Bi atoms donate one electron per atom in the condition band are simultaneously plotted against the composition in the inset of Fig. 7. In the normal metallic region, i.e.,

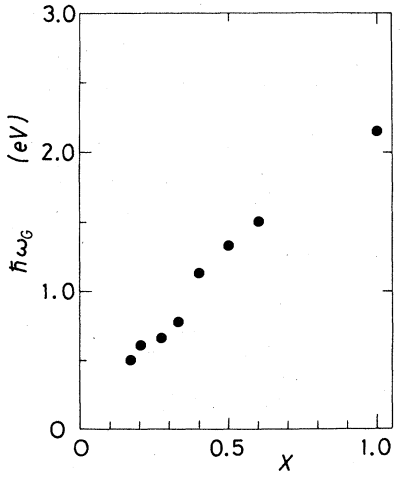

FIG. 6. Composition (x) dependence of the peak-position energy in the conductivity spectrum $\sigma_1(\omega)$.

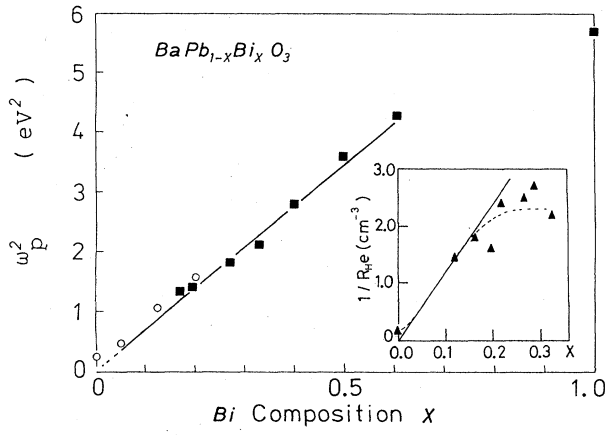

FIG. 7. Composition (x) dependence of the square of the plasma frequency ω_p. In the inset the carrier densities estimated from the Hall effect are plotted. The solid line in the inset is calculated on the assumption that Bi atoms donate one electron per atom in the conduction band.

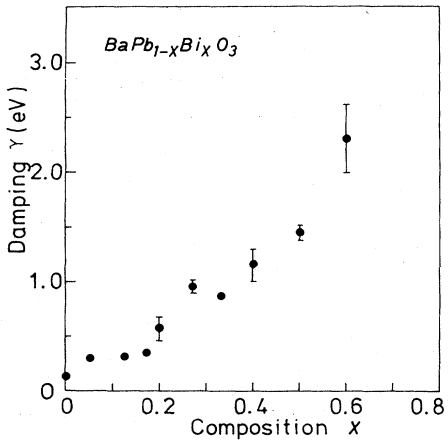

FIG. 8. Composition (x) dependence of the optical damping obtained by the curve fitting. The error bar represents the difference between the best-fit parameters obtained using the Drude equation [Eq. (1)] and by using Eq. (4).

$0<x<0.17$, the electrically estimated carrier density also seems to vary linearly with x, while it shows saturation in the compositional range $x>0.17$, where the reflectivity spectrum deviates from the Drude curve. These results indicate that this material is no longer a normal metal in the compositional range $0.15<x<0.35$, and nevertheless the electrons supplied by Bi atoms take part in the optical collective excitation in the wider compositional range including the semiconducting phase.

In Fig. 8 the damping factor of the collective excitation obtained by the fitting calculation is plotted against the composition. Roughly speaking, the damping γ seems to increase linearly with x, that is, γ seems to be proportional to the Bi content. In Fig. 9 the two kinds of conductivity are plotted for comparison. One of them is measured electrically[8] and the other is estimated optically. The latter is defined as $\sigma(0)=\omega_p^2\epsilon_\infty/\gamma$, each parameter ω_p, $\epsilon\infty$, and γ being obtained by the Drude fit in the higher-energy region. In the normal-metal compositional range the values of the two are almost equal, whereas the electrical conductivity begins to decrease rapidly at about $x\simeq 0.33$, corresponding to the deviation from the Drude model. It is remarkable that the optical conductivity is almost constant over the wide compositional range, which shows that increase of ω_p^2 is compensated by an increase of γ in determining the conductivity. This suggests that Bi acts as a donor impurity and as a normal scattering center simultaneously. From Figs. 8 and 9 it is concluded that this material appears to be essentially, a metal with simple band structure in the energy region of around 1 eV or higher, while in the low-energy region an appreciable deviation from the simple metal develops with increasing x.

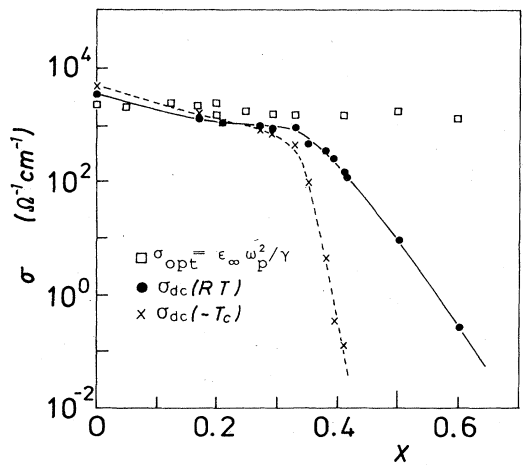

FIG. 9. Composition (x) dependence of the zero-frequency conductivity. The data indicated by ● and × are the dc conductivities measured electrically. The data indicated by □ are the optical conductivities obtained by extrapolating the measurement spectrum towards lower energy based on the Drude theory.

IV. DISCUSSIONS

A. Metallic phase

As shown in Fig. 4, the alloys with composition $x<0.35$ can be classified as metals from the optical spectrum. Although the alloys with $x>0.15$ show deviation from the normal-metal behavior, the plasma edge is clearly observed in the spectrum and the reflectivity continues to increase towards perfect reflection as $\omega\rightarrow 0$. As demonstrated in Figs. 2 and 5, the reflectivity and the optical conductivity for the alloys with $x<0.15$ can be fitted to the Drude-type frequency dependences. The normal metallic properties in the above compositional range have also been confirmed by other measurements, in particular, by the electrical measurements. The carrier density estimated from the Hall coefficient yields a value corresponding to one electron per Bi atom.[23] The Seebeck coefficient is found to increase linearly with the temperature—the typical metallic behavior—for the samples in the same compositional range.[9]

We have already reported as a preliminary result that the plasma frequency ω_p defined by the reflectivity edge increases with increasing x for the ceramic specimens.[21] It was found that ω_p^2 varies almost linearly with x. The present measurements, made on single crystalline specimens, have also confirmed the relation $\omega_p^2\propto x$ in the wide compositional range, which suggests that homogeneous solid solutions are formed over the entire range we have investigated. Since ω_p^2 is proportional to the free-electron density as shown in Eq. (3), this fact indicates that the Bi concentration n_{Bi} is proportional to the free-electron density n. Considering the results for the Hall coefficient which indicate $n=n_{\mathrm{Bi}}$ at $x=0.12$, we may conclude that Bi atoms donate one electron per atom to the conduction band of $BaPbO_3$ over the whole compositional range.

It should also be noted that the optical dielectric constant, which is determined from the reflectivity in the frequency region above the reflectivity edge, i.e., ω_p, does not change appreciably over the whole range of x: $\epsilon_\infty=5\pm 1$ for all the samples measured. This result implies that the electronic structure involved in the higher-energy excita-

tions does not change appreciably in the entire alloy series. Based on the constant ϵ_∞, the linear relationship between ω_p^2 and x leads to an effective mass m^* independent of x. From the slope of the line in Fig. 7, we estimate $m^* \simeq 0.5 m_e$ using the value $\epsilon_\infty = 5$ with m_e being the free-electron mass. Note that m^* is the so-called optical effective mass which is independent of the detailed electronic structure in the low-energy region ($\omega < \omega_p$) such as the effect of electron-phonon interaction or the energy gap in the vicinity of the Fermi energy due to CDW instability. In fact this value is smaller, by a factor of about 2, than the electron mass estimated from the result of the Seebeck effect for the samples in the metallic phase.[9] Considering the fact that the latter is subjected to phonon dressing, we can say that the agreement between the two is fairly good.

A priori band-structure calculations of Mattheiss and Hamann yielded a very similar value ($\sim 0.5 m_e$) for the effective mass in the conduction band of the $BaPb_{1-x}Bi_xO_3$ alloy series.[4,24] According to their calculation the energy bands near the Fermi energy are composed of a hybridized set of states derived from the 6*s* levels of the Pb or Bi ions and the 2*p* levels of the O ions. The 6*s*-2*p* complex forms a very broad band with a total width of around 16 eV. Since a rather light band mass is a natural consequence of the *s*-*p*—derived bands, the present result strongly supports the result of the band calculations as far as the energy region near ω_p or higher is concerned. It should also be noted that the effective mass in the present system is smaller by more than an order of magnitude than that for other systems showing relatively high-T_c superconductivity, such as in *A*15 and Chevrel-phase compounds where the *d*- or *f*-derived bands play an essential role.[25]

B. Semiconducting phase

The reflectivity spectrum in the semiconducting phase ($x > 0.35$) is characterized by optical phonons in the low-frequency region and by the reflectivity edge observed at high frequencies. The attempt to extract information on the semiconducting phase from the phonon spectrum is reported elsewhere. Here, we discuss the electronic structure of the alloys in the semiconducting phase deduced from the optical spectrum.

As shown in Fig. 5, a pronounced maximum appears in the optical conductivity spectrum in the higher-energy region. This peak has the most spectral weight in the energy range up to about 3 eV and therefore is assigned to electronic transitions between energy bands separated by an energy gap. Note that we do not see a square-root edge, i.e., $(\hbar\omega - E_G)^{1/2}$, typical for the interband transition of ordinary semiconductors such as GaAs. The structure in the present case rather resembles the interband transitions in narrow-band materials or the transitions across a Peierls gap in CDW systems such as KCP (Ref. 26) and $K_{0.3}MoO_3$ (Ref. 27).

The reflectivity edge observed at the higher energy denoted also by ω_p should correspond to a longitudinal collective excitation associated with the interband transitions which give rise to a conductivity peak. A notable result is that the values of ω_p sit almost on a single line, $\omega_p^2 = Kx$, extrapolated from the metallic phase. This strongly suggests that the electronic states involved in the interband transitions are those derived from the one excess valence electron on the Bi atom. The same states contribute to the free-carrier plasma in the metallic phase. In the end member, $BaBiO_3$, the 6*s* level hybridized with the $2p_z$ level of the O atom forms a set of bands near the Fermi level, as is also the case in $BaPbO_3$. The Fermi level should be located in the middle of the upper 6*s*-2*p* band in the case of $BaBiO_3$. In the actual material the lattice distortions, predominantly the breathing-mode distortions, make the system semiconducting by creating a gap near the Fermi level—the CDW instability. The experimental facts indicate that the same mechanism is responsible for the semiconductivity of the alloys and that the interband transitions are between the split-off Bi bands.

The effect of alloying is seen in the downward shift of the conductivity-peak position with increasing Pb composition as shown in Fig. 5. This can be interpreted as the decrease in the separation between the Bi split-off bands. There seems to be no explicit role of Pb in the electronic structure of the alloys in the semiconducting phase. However, the resistivity data suggests the presence of the Pb states in the energy-gap region.[8] The activation energy that determines the low-temperature resistivity is small and obviously different from that in the high-temperature region. Besides, the low-temperature activation energy is found to decrease towards zero at $x_c \simeq 0.35$ with increase of Pb composition, possibly due to the increasing weight or width of the Pb states in the gap. Hence, the plasma dominating in the low-energy region of the room-temperature spectrum for $x = 0.4$ may originate from carriers thermally activated in the same states.

C. Metal-semiconductor transition and precursor effect

Based on the discussions in the preceding sections the models for the electronic structure in the metallic and semiconducting phase are depicted schematically in Figs. 10(a) and 10(c), respectively. Extrapolation of the energy scheme from the semiconducting side naturally leads to a metal-semiconductor transition. Since the splitting of the Bi band seems to decrease with increase of Pb composition, corresponding to the shift of the conductivity maximum towards lower energy as shown in Fig. 5, eventually the lower split-off Bi band will overlap with the Pb band at a certain x. We consider that this takes place at around $x = 0.35$.

The splitting of the Bi band is substantially larger even near the critical composition as deduced from the position of the optical conductivity peak, e.g., at 1.1 eV for $x = 0.4$ (Fig. 6). So it is likely that the splitting remains even in the metallic phase. Indeed a peak, although not so pronounced as in the semiconducting phase, shows up in the $\sigma_1(\omega)$ spectrum even for the metallic samples with Bi composition greater than 0.17 as shown in Fig. 5 and the peak positions are at the energies extrapolated from the semiconducting phase. From this we can imagine the electronic structure as shown in Fig. 10(b) for the alloys in the range $0.15 < x < x_c$ (~ 0.35).

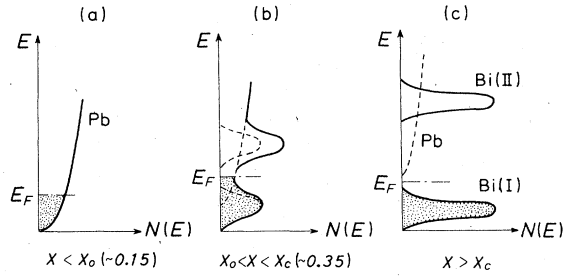

FIG. 10. Schematic band model of $BaPb_{1-x}Bi_xO_3$ based on our experimental results. (a) Normal-metal region: The Fermi level shifts upwards gradually as x increases. (b) Transition region: The split-off Bi bands overlap the Pb band and the Fermi level is pinned between these Bi bands. (c) Semiconducting region: The Pb band is separated from the lower split-off Bi band. The Fermi level is located between these two bands.

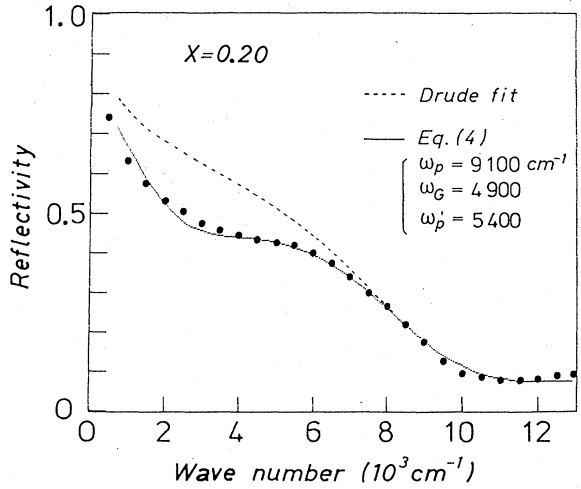

FIG. 11. Curve fitting by the Drude equation [Eq. (1)] and by Eq. (4).

In the above energy-band scheme for $0.15 < x < x_c$ the Fermi level which crosses the Pb band is pinned at a position midway between the split-off Bi bands. Therefore, the number of electronic states near the Fermi energy available for the dc or low-energy properties does not increase even with increase of Bi concentration. This is in agreement with the experimental observations such as Hall[5,8] and Seebeck effects,[9] in which the carrier density and the Fermi energy are observed to saturate. The recent transport measurement by Suzuki and Murakami[28] has suggested the coexistence of the metallic carriers, the number of which is independent of temperature, with the thermally activated carriers for single-crystalline thin films in the metallic compositional range. This result can also be interpreted in terms of the electronic structure proposed here.

We should remark that the reflectivity spectrum for the alloys $x > 0.15$ can be simulated fairly well by assuming the following dielectric function:

$$\epsilon(\omega)=\epsilon_\infty\left[1+\frac{\omega_p^2-\omega_G^2}{\omega_G^2-\omega^2-i\omega\gamma}-\frac{\omega_p'^2}{\omega^2+i\omega\gamma'}\right]. \quad (4)$$

Here, the second term is introduced to represent the interband excitations across a gap ω_G and the associated reflectivity edge at ω_p. The third term represents the metallic contribution due to the finite Fermi surface after the splitting of the Bi band in the metallic phase or to the carriers thermally activated in the semiconducting phase. All the experimental data can be fitted to the curves calculated using the above dielectric function. One example is shown in Fig. 11. Thus, this fitting procedure yields more reliable values for the parameters ω_p, ω_G, and γ. The obtained parameters ω_p and γ do not differ significantly from the values determined by the original Drude fit and the value of ω_G is found to coincide with the peak position of $\sigma_1(\omega)$. It is rather surprising that the second term in Eq. (4) can describe the interband transitions in the present system consisting of the bands derived only from s and p levels. Such a simple formula is usually appropriate for the interband transitions between narrow f and d bands. One may therefore postulate that the density of states associated with Bi bands has a narrow maximum in contrast to the broad Pb band, which might be a reason why the Bi bands manifest themselves even if they overlap with the Pb band in the metallic phase.

As we briefly described before, the properties in this regime at first glance appear to be determined by the macroscopic phase separation or inhomogeneity in the crystals. If a sudden transformation were to take place at around $x=0.35$ from the electronic structure shown in Fig. 10(c) to that in Fig. 10(a), then the transition should have been of first order. In this case, as Mott frequently points out,[29] a phase separation is an inevitable consequence although somehow dependent on the conditions of the crystal growth. Takagi *et al.*[12] have recently observed the coexistence of superconductivity, but only in tiny volume fraction, in the semiconducting single crystals. However, such observation is in the narrow compositional range restricted between 0.35 and 0.40. On the other hand, unusual properties, such as, non-Drudian optical spectrum, start to show up already at $x \sim 0.15$. Therefore, it is more appropriate to regard this regime as a precursory one that bridges the metallic and semiconducting phase without any abrupt change in the electronic structure.

D. Relevance to the available theories

Here, we discuss the physical grounds for the electronic structure of $BaPb_{1-x}Bi_xO_3$ proposed in the preceding sections. The model shown in Fig. 10(a) is identical to that proposed by Mattheiss and Hamann (MH) from LAPW band calculation.[4] For the end member $BaPbO_3$ the observation of a plasma edge in the infrared region gives clear evidence for the semimetallic state of this material, which is in agreement with the result of MH, predicting a small band overlap between the Pb $6s$ and the O $2p$ nonbonding bands. They used the virtual-crystal approximation for the electronic structure of the alloys. The present experiments have also yielded support for such a rigid band picture at least up to the Bi composition $x \sim 0.1$. Notably, the estimated effective mass of the conduction electrons, which is found to be rather small, $m^*/m_e \simeq 0.5$,

is reasonable in view of the band arising from the atomic s and/or p orbitals.

If one extrapolates the rigid-band scheme to the opposite end member $BaBiO_3$, this material should be a metal with the Fermi level in the middle of the Bi 6s conduction band. MH proposed that the breathing-mode distortion of the O lattice is responsible for the semiconductivity. The distortion makes neighboring Bi sites inequivalent and the Fermi surface would be perfectly nesting in the case of a half-filled tight-binding band. Thus, one expects a semiconducting CDW ground state for $BaBiO_3$. However, such a long-range CDW state will be destroyed easily by alloying with Pb. In order to explain the semiconductivity of the alloys in a rather wide compositional range, the model proposed by Rice and Sneddon (RS) seems to be more appropriate.[14] They presumed an attractive interaction mediated by the breathing-mode phonons and localized on Bi sites (Anderson negative U).[30] The model emphasizes the local nature of the CDW instability. The CDW state would then be stable against alloying with Pb and the semiconducting phase would persist over a wide compositional range. In addition, Rice suggested that static disordered distortions of the O atoms would remain even in the metallic phase and they would strongly modify the metallic properties.[31]

As they themselves pointed out, the RS model needs to be extended to the case of finite bandwidth. Recently, Yoshioka and Fukuyama (YF) have proposed a model describing a superconductor-semiconductor transition for a binary-alloy system.[15] The essential point of the model is that explicit account is taken of the site-energy difference as well as of the one-site attractive interaction. The on-site attraction enhances the effective site-energy difference. Hence, a metal-semiconductor transition takes place when the effective site-energy difference exceeds the bandwidth. The model leads to a conclusion similar to that of the RS model when it is applied to the present system. In this case an energy gap will be created at the transition between the Pb 6s band and the lower split-off Bi 6s band. This is essentially the same as the energy scheme we have drawn in the preceding section.

Even in the metallic phase, the YF model predicts the presence of a dip in the density of states near the Fermi level just like that shown in Fig. 10(b). If the on-site attractive interaction is localized only on the Bi site, the magnitude of negative U will be an increasing function of the Bi composition. Then, the increase in the Bi composition will enhance both the effective site-energy difference and the splitting of the Bi band as is observed in the experiments. The enhanced differences in site energy would make a structure in the density of states as shown in Fig. 10(b), which will become progressively pronounced with increasing Bi content and the transition to the semiconducting state will result.

The regime depicted in Fig. 10(b) is analogous to the precursor or fluctuation regime in the case of Peierls instability.[26,27] This is seen at temperatures above the onset of the CDW long-range order, and a minimum in the density of states, a pseudogap, appears in the electronic spectrum. In a separate paper[6] we have been led, through consideration of the far-infrared phonon spectrum, to the conclusion that long-range order in the present system corresponds to the charge disproportionation state of Bi atoms. As is widely accepted for $BaBiO_2$, the Bi atoms form a superlattice composed of a three-dimensional alternating array of two inequivalent Bi sites, i.e., [—Bi(I)—Bi(II)—], configurations where Bi(I) and Bi(II) represent differently charged Bi atoms. This superstructure is considered to be introduced by the condensation of the breathing-mode phonons. Assuming that the Bi composition x plays a role similar to that of the temperature in the case of the Peierls instability, the precursor regime would then be originated due to the local fluctuation of the Bi content in the alloy, which possibly leads to the formation of clusters with [—Bi(I)—Bi(II)—] short-range order.

V. SUMMARY

Based on the results of the optical spectra we have developed a picture for the electronic structure of $BaPb_{1-x}Bi_xO_3$ as summarized below. This picture explains quite well not only the observed optical properties, but also the extensive electronic transport properties.

(a) When the Bi content is low, up to about 10 at. %, Bi donates one electron per atom to the Pb conduction band. Therefore, the alloys in this compositional range show normal metallic behavior as confirmed by the Drude-like optical spectra and other experimental observations.

(b) At or beyond $x=0.1$, the distinction between Bi 6s and Pb 6s states becomes appreciable and simultaneously, the Bi band is split due to the breathing-mode distortions localized on Bi sites. But still a finite density of states near the Fermi level remains, due to the band overlap between Pb and the lower Bi split-off bands, although it is depressed appreciably. This is clearly seen in the reduced but finite optical conductivity in the low-energy region. Following this change the interband transition between the two Bi split-off bands starts to dominate in the spectrum in the higher-energy region. This effect manifests itself as a reflectivity edge and also as a peak feature in the real part of the optical conductivity. The position of the reflectivity edge shifts to higher energy with increasing Bi content, corresponding to the increase in the number of available states for the interband transitions.

(c) With further increase of Bi content the conductivity peak shifts towards higher energy, which corresponds to the increase in the splitting of the Bi 6s band. In association the Pb 6s band is pushed upward relative to the Bi 6s band and finally a complete gap opens. The optical spectrum of the semiconducting phase is characterized by low-energy phonons and a high-energy interband transition across a gap created in the Bi 6s bands. The optical conductivity shows a pronounced peak corresponding to the interband transition which is quite different from a square-root edge observed in the usual semiconductors but rather resembles the spectrum of the material showing Peierls instability.

The regime (b) exactly corresponds to that of high-T_c superconductivity. Hence it is likely that a strong electron-phonon interaction is responsible for both superconductivity and the local instability towards the semiconducting states. However, it is not so clear if both of

them come about because of the coupling with a single specific phonon, e.g., the breathing-mode phonon.

ACKNOWLEDGMENTS

We would like to thank Dr. S. Sugai at Osaka University, Japan, for his help in measuring a part of the far-infrared spectra and in carrying out the calculation of the Kramers-Kronig transformation. We also thank Professor T. M. Rice at Eidgenössische Technische Hochshule, Hönggerberg, Zürich, and Dr. D. Yoshioka at Kyushu University, Japan, for their helpful discussions. This work was supported by the Japanese Ministry of Education, Science and Culture.

[1]A. W. Sleight, J. L. Gillson, and P. E. Bierstedt, Solid State Commun. **17**,27 (1975).
[2]B. Batlogg, Physica **126B**, 275 (1984), and references therein.
[3]K. Kitazawa, M. Naito, T. Itoh, and S. Tanaka, J. Phys. Soc. Jpn. **54**, 2682 (1985).
[4]L. F. Mattheiss and D. R. Hamann, Phys. Rev. B **26**, 2686 (1982); **28**, 4227 (1983).
[5]T. D. Thanh, A. Koma, and S. Tanaka, Appl. Phys. **22**, 205 (1980).
[6]S. Uchida, S. Tajima, A. Masaki, S. Sugai, K. Kitazawa, and S. Tanaka, J. Phys. Soc. Jpn. (to be published).
[7]B. Batlogg, J. P. Remeika, R. C. Dynes, H. Barz, A. S. Cooper, and J. P. Garno, in *Superconductivity in d- and f-band Metals,* edited by W. Buckel and W. Weber (Kernforschungszentrum, Karlsruhe, 1982), p. 401.
[8]H. Takagi, M.S.c. thesis, University of Tokyo, 1985.
[9]T. Tani, T. Itoh, and S. Tanaka, J. Phys. Soc. Jpn. Suppl. A **49**, 309 (1980).
[10]T. Itoh, K. Kitazawa, and S. Tanaka, J. Phys. Soc. Jpn. **53**, 2668 (1984).
[11]A. Katsui, Y. Hidaka, H. Takagi, J. Cryst. Growth **66**, 228 (1982).
[12]H. Takagi, M. Naito, S. Uchida, K. Kitazawa, S. Tanaka, and A. Katsui, Solid State Commun. **55**, 1019 (1985).
[13]K. Kondo and E. Hanamura, Research Report on New Superconducting Materials, Special Project No. 106, Ministry of Education, Science and Culture, 1985 (unpublished).
[14]T. M. Rice and L. Sneddon, Phys. Rev. Lett. **47**, 689 (1981); Physica **107B**, 661 (1981).
[15]D. Yoshioka and H. Fukuyama, J. Phys. Soc. Jpn. **54**, 2996 (1985).
[16]A. S. Barker, J. A. Ditzenberger, and F. J. DiSalvo, Phys. Rev. B **12**, 2049 (1975).
[17]A. S. Barker and J. P. Remeika, Solid State Commun. **8**, 1521 (1970).
[18]J. Th. W. de Hair and G. Blasse, Solid State Commun. **12**, 727 (1973).
[19]Y. Khan, K. Nahm, M. Rosenberg, and H. Willner, Phys. Status Solidi A **39**, 79 (1977).
[20]S. Sugai, S. Uchida, K. Kitazawa, S. Tanaka, and A. Katsui, Phys. Rev. Lett. **55**, 426 (1985).
[21]S. Tajima, K. Kitazawa, and S. Tanaka, Solid State Commun. **47**, 659 (1983).
[22]C. Methfessel and M. Methfessel, in *Superconductivity in d- and f-band Metals,* Ref. 7, p. 393.
[23]K. Kitazawa, A. Katsui, A. Toriumi, and S. Tanaka, Solid State Commun. **52**, 459 (1984).
[24]L. F. Mattheiss, Phys. Rev. B **28**, 6629 (1983).
[25]J. A. Woolam and S. A. Alterovitz, Phys. Rev. B **19**, 749 (1979).
[26]P. Bruesch, S. Strassler, and H. R. Zeller, Phys. Rev. B **12**, 219 (1975).
[27]G. Travaglini and P. Wachter, Phys. Rev. B **30**, 1971 (1984).
[28]M. Suzuki and T. Murakami, Solid State Commun. **53**, 691 (1985).
[29]See, for example, N. F. Mott, Philos. Mag. B **50**, 161 (1984).
[30]P. W. Anderson, Phys. Rev. Lett. **34**, 953 (1975).
[31]T. M. Rice, in *Superconductivity in Magnetic and Exotic Materials,* edited by T. Matsubara and A. Kotani (Springer, Berlin, 1984), p. 178; and private communication.